



# Magnetocaloric effect and critical behaviors of $R_2\text{NiMnO}_6$ ( $R=\text{Eu}$ and $\text{Dy}$ ) double perovskite oxides

Lei Su <sup>a, b</sup>, Xiang-Qun Zhang <sup>b</sup>, Qiao-Yan Dong <sup>c, \*\*</sup>, Ya-Jiao Ke <sup>b</sup>, Kai-Yue Hou <sup>b, c</sup>,  
Cheng-Shi Liu <sup>a</sup>, Zhao-Hua Cheng <sup>b, \*</sup>

<sup>a</sup> Key Laboratory for Microstructural Material Physics of Hebei Province, School of Science, Yanshan University, Qinhuangdao 066004, PR China

<sup>b</sup> Key Laboratory for Magnetism, Institute of Physics, Chinese Academy of Sciences, Beijing 100190, PR China

<sup>c</sup> Center for Condensed Matter & Beijing Key Laboratory of Metamaterials and Devices, Department of Physics, Capital Normal University, Beijing 100048, PR China

## ARTICLE INFO

### Article history:

Received 5 January 2018

Received in revised form

26 February 2018

Accepted 27 February 2018

Available online 6 March 2018

### Keywords:

Ceramics

Magnetization

Magnetocaloric

Critical behavior

## ABSTRACT

We have investigated the magnetocaloric effects and critical behaviors of  $\text{Eu}_2\text{NiMnO}_6$  and  $\text{Dy}_2\text{NiMnO}_6$  double perovskite oxides. For a magnetic field varying from 0 to 7 T, the maximum values of the magnetic entropy change ( $|\Delta S_M^{\max}|$ ) reach 4.0 J/kg K and 5.2 J/kg K, and the relative refrigeration capacity (RCP) values are 241.5 J/kg and 385.1 J/kg for  $\text{Eu}_2\text{NiMnO}_6$  and  $\text{Dy}_2\text{NiMnO}_6$ , respectively. The relatively high values of  $|\Delta S_M|$  and RCP suggest that these double perovskite oxides can be used as candidates of magnetic refrigerants working in a wide temperature range. Various techniques such as modified Arrott plot, Kouvel-Fisher method and critical isotherm analysis are used to estimate the critical exponents ( $\beta$ ,  $\gamma$  and  $\delta$ ) as well as  $T_C$  for  $\text{Eu}_2\text{NiMnO}_6$ . These critical exponents not only obey the Widom scaling relation  $\delta = 1 + \gamma/\beta$ , but also fulfill the scaling equation  $M(H, \epsilon) = \epsilon^\beta f_\pm(H/\epsilon^{\beta+\gamma})$  where  $\epsilon = (T - T_C)/T_C$ ,  $f_+$  ( $T > T_C$ ) and  $f_-$  ( $T < T_C$ ) are the regular analytic functions. Therefore, the deduced critical exponents are reasonably accurate. Moreover, temperature variation in effective critical exponents resemble with those for disordered ferromagnet, which matches with the Griffiths-like phase behavior observed from inverse magnetic susceptibility just above  $T_C$ .

© 2018 Published by Elsevier B.V.

## 1. Introduction

In recent years, with the constantly increasing need for powerful, clean, efficient, and miniaturized devices incorporating different physical properties, much attention has been attracted to double perovskite oxides as multifunctional materials because they simultaneously possess magnetic, dielectric, magnetodielectric and magnetocaloric (MC) properties [1–5]. This kind of oxides have general stoichiometric formula  $A_2B'B''\text{O}_6$ , where A is rare-earth, alkali or alkaline-earth ion and B', B'' are transition metal ions [6].  $\text{La}_2\text{NiMnO}_6$  is a typical one of them. There are abundant reports on its magnetic and magnetocaloric properties [7,8], magnetodielectric properties [9], magnetocapacitance and magnetoresistance [10].

\* Corresponding author.

\*\* Corresponding author.

E-mail addresses: [dongqy@cnu.edu.cn](mailto:dongqy@cnu.edu.cn) (Q.-Y. Dong), [zhcheng@iphy.ac.cn](mailto:zhcheng@iphy.ac.cn) (Z.-H. Cheng).

$\text{La}_2\text{NiMnO}_6$  shows a ferromagnetic (FM)-paramagnetic (PM) phase transition around Curie temperature ( $T_C$ ) of 280 K [11].  $\text{Ni}^{2+}-\text{O}-\text{Mn}^{4+}$  superexchange interaction leads to the appearance of FM state [12]. For magnetocaloric effect (MCE), Monte Carlo simulations have proved the temperature where the maximum of the magnetic entropy change locates is in accord with  $T_C$  [13]. Furthermore, modulating the coupling between the spin and phonon have greatly enhanced the magnetic entropy change of polycrystalline  $\text{La}_2\text{NiMnO}_6$  [7].

On the basis of the magnetocaloric effect, magnetic refrigeration as a promising technology compared with the traditional gas-compression refrigeration because of its higher efficiency and environmentally friendly has attracted more attentions [14,15]. It is of great significance to explore new magnetic refrigeration materials. Recently, the double perovskite family of  $R_2\text{NiMnO}_6$  ( $R = \text{Pr}$ ,  $\text{Nd}$ ,  $\text{Tb}$ ,  $\text{Ho}$ , and  $\text{Y}$ ) have been found they possess considerably high values of  $|\Delta S_M|$  and RCP as the prospective magnetocaloric refrigerant around  $T_C$  [4]. Subsequently,  $\text{Dy}_2\text{NiMnO}_6$  is also thought as a promising magnetic refrigerant material because it shows amazing

magnetocaloric effect in a wide temperature range [16]. In addition, many Eu-based oxides such as  $\text{EuHo}_2\text{O}_4$  and  $\text{EuDy}_2\text{O}_4$  [17],  $\text{Eu}_{1-x}\text{Ba}_x\text{TiO}_3$  ( $0.1 \leq x \leq 0.9$ ) [18],  $\text{EuTiO}_3$  [19] have been reported to exhibit a large magnetic entropy change. Within this context, we report the magnetocaloric effect of  $\text{R}_2\text{NiMnO}_6$  ( $\text{R} = \text{Eu}$  and  $\text{Dy}$ ) polycrystalline samples. At the same time, we also systematically investigate the critical behavior of  $\text{Eu}_2\text{NiMnO}_6$  for a better understanding of its magnetic transition.

## 2. Experimental process

Polycrystalline  $\text{Eu}_2\text{NiMnO}_6$  and  $\text{Dy}_2\text{NiMnO}_6$  were synthesized by standard solid-state reaction method. Stoichiometric amounts of  $\text{R}_2\text{O}_3$  ( $\text{R} = \text{Eu}$  or  $\text{Dy}$ ) (purity of 99.99 wt %),  $\text{NiO}$  (purity of 99.998%) and  $\text{MnO}_2$  (purity of 99.9 wt %) were intensively mixed. The mixtures for  $\text{Eu}_2\text{NiMnO}_6$  and  $\text{Dy}_2\text{NiMnO}_6$  samples were calcined at  $1000^\circ\text{C}$  for 24 h and  $1200^\circ\text{C}$  for 24 h under the atmosphere of air, respectively. Then they were cooled down to room temperature in the furnace at the rate of  $1^\circ\text{C}/\text{min}$ . Consecutively, the resulting powders were reground, pressed into pellets and sintered at  $1200^\circ\text{C}$  for 24 h for  $\text{Eu}_2\text{NiMnO}_6$  and at  $1300^\circ\text{C}$  for 24 h for  $\text{Dy}_2\text{NiMnO}_6$ . Powder X-ray diffractometer (Rigaku Ultima-IV diffractometer with combined  $\text{Cu-K}\alpha$  radiation) was performed to characterize the crystal structure of the samples. The dc magnetic measurements were carried out on a superconducting quantum interference device magnetometer (MPMS XL, Quantum Design) in magnetic fields up to 7 T at temperatures between 2 K and 300 K.

## 3. Results and discussion

### 3.1. Structural properties

Rietveld refined powder X-ray diffraction (XRD) patterns of  $\text{Eu}_2\text{NiMnO}_6$  and  $\text{Dy}_2\text{NiMnO}_6$  polycrystalline samples at room temperature (See Fig. 1) show that the  $\text{Eu}_2\text{NiMnO}_6$  sample is in pure phase with a monoclinic structure (space group  $\text{P}2_1/\text{n}$ ), while  $\text{Dy}_2\text{NiMnO}_6$  sample has the main phase with a monoclinic structure (space group  $\text{P}2_1/\text{n}$ ) as well as a small amount of impurity phase  $\text{Dy}_2\text{O}_3$  marked by “↓” in the pattern of Fig. 1. The obtained structural and reliability parameters of  $\text{Eu}_2\text{NiMnO}_6$  and  $\text{Dy}_2\text{NiMnO}_6$ , as well as  $\text{La}_2\text{NiMnO}_6$  [20,21], are shown in Table 1. The lattice parameters of  $\text{Eu}_2\text{NiMnO}_6$  and  $\text{Dy}_2\text{NiMnO}_6$  are in accord with the previous

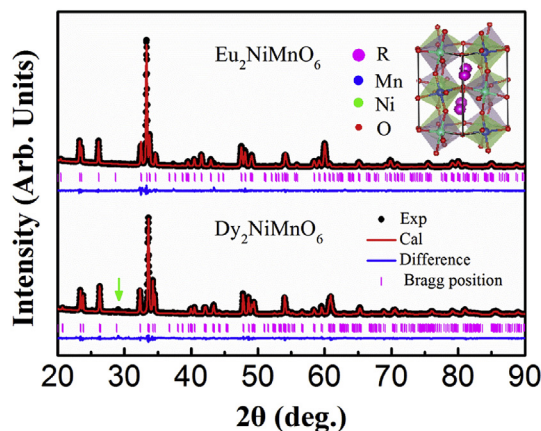


**Fig. 1.** Rietveld refined powder XRD patterns of  $\text{Eu}_2\text{NiMnO}_6$  and  $\text{Dy}_2\text{NiMnO}_6$  at room temperature. The experimental data are indicated by dots, and the calculated profile is shown by the solid line. The short vertical lines show the positions of the Bragg diffraction peak. The underneath curve shows the difference between the observed and calculated intensity. The inset shows the crystallographic structure of  $\text{R}_2\text{NiMnO}_6$ .

**Table 1**

Structural and reliability parameters obtained from the refinement for  $\text{R}_2\text{NiMnO}_6$  ( $\text{R} = \text{Eu}$  and  $\text{Dy}$ ) as well as  $\text{La}_2\text{NiMnO}_6$  [20,21].

	$\text{La}_2\text{NiMnO}_6$	$\text{Eu}_2\text{NiMnO}_6$	$\text{Dy}_2\text{NiMnO}_6$
$a$ (Å)	5.5115	5.3249	5.2466
$b$ (Å)	5.4851	5.5282	5.5500
$c$ (Å)	7.7387	7.5873	7.5055
$V$ (Å <sup>3</sup> )	232.79	223.35	218.55
$\beta$ (°)	90.015(2)	90.008(1)	90.251(7)
Bond angles(°)			
Ni–O <sub>1</sub> –Mn	157.6(1)	149.4(2)	143.2(7)
Ni–O <sub>2</sub> –Mn	163.5(9)	145.0(3)	148.8(8)
Ni–O <sub>3</sub> –Mn	160.9(1)	150.8(2)	149.4(6)
⟨Ni–O–Mn⟩	160.7(1)	148.4(2)	147.2(0)
Average bond length(Å)			
⟨Ni–O⟩	1.97(3)	2.01(2)	1.95(5)
⟨Mn–O⟩	1.96(2)	1.96(2)	2.00(4)
R:x	0.0021(6)	0.5108(9)	0.5168(3)
y	0.0171(2)	0.5590(1)	0.5692(5)
z	0.2524(7)	0.2483(8)	0.2517(3)
Ni:x y z	0 1/2 0	1/2 0 0	1/2 0 0
Mn:x y z	1/2 0 0	0 1/2 0	0 1/2 0
O <sub>1</sub> :x	−0.218(5)	0.2257(9)	0.1901(4)
y	0.191(5)	0.2160(8)	0.1895(0)
z	−0.019(4)	0.9373(5)	0.9415(9)
O <sub>2</sub> :x	0.233(4)	0.3238(8)	0.3140(0)
y	0.758(4)	0.6892(9)	0.7141(4)
z	0.466(3)	0.9582(1)	0.9509(3)
O <sub>3</sub> :x	0.559(2)	0.4108(3)	0.4019(8)
y	−0.001(1)	0.9775(7)	0.9694(3)
z	0.265(3)	0.2698(0)	0.2551(3)
$R_p$	7.93	1.90	1.48
$R_{wp}$	10.8	2.95	2.04
$\chi^2$	3.47	7.99	5.14

works [22,23]. As summarized in Table 1, lattice parameters  $a$  and  $c$ , cell volume  $v$ , and ⟨Ni–O–Mn⟩ bond angle  $\psi$  decrease, while lattice parameter  $b$  increases with decreasing the lanthanide ionic radius. Refinement parameter  $\chi^2$  is defined as  $R_{wp}/R_{exp}$ , where  $R_{wp}$  is the weighted-profile  $R$  value,  $R_{exp}$  is the statistically expected  $R$  value and reflects the quality of the data (*i.e.* the counting statistics) [24]. Ideally,  $\chi^2$  should approach 1. However, the  $\chi^2$  values of  $\text{Eu}_2\text{NiMnO}_6$  and  $\text{Dy}_2\text{NiMnO}_6$  polycrystalline samples are much larger than 1. There are two reasons. One is that the XRD data have been over-collected which results a small  $R_{exp}$  value. The other is a large  $R_{wp}$  value due to the level of background when collecting XRD data.

### 3.2. Magnetic properties

In order to confirm the magnetic properties of  $\text{Eu}_2\text{NiMnO}_6$  and  $\text{Dy}_2\text{NiMnO}_6$  oxides, the temperature ( $T$ )-dependence of magnetization ( $M$ ) has been measured. Fig. 2(a)–(b) show the zero field cooling (ZFC) and field cooling (FC) magnetization vs. temperature curves of  $\text{Eu}_2\text{NiMnO}_6$  and  $\text{Dy}_2\text{NiMnO}_6$  from 2 K to 300 K under 0.01 T. With increasing the temperature, it is evident that the compounds undergo a ferromagnetic-paramagnetic phase transition. The Curie temperature  $T_C$ , corresponding to the maximum slope of FC  $M$ - $T$  curve ( $|dM/dT|$ ) (See the insets of Fig. 2(a)–(b), is determined to be 145 K for  $\text{Eu}_2\text{NiMnO}_6$  and 97 K for  $\text{Dy}_2\text{NiMnO}_6$ , respectively. They are in agreement with the result reported in the literatures [22,23]. The  $T_C$  of  $\text{La}_2\text{NiMnO}_6$  reported is 280 K [11]. Obviously,  $T_C$  shifts towards low temperature with decreasing the lanthanide ionic radius. It also can be seen from Fig. 2(a)–(b) that the ZFC and FC curves are completely reversible around  $T_C$ . However, a significant thermal magnetic irreversibility between the ZFC and FC branches is clearly observed below  $T_C$ . This kind of bifurcation is also yielded in many other  $\text{R}_2\text{NiMnO}_6$  compounds such as

Download English Version:

<https://daneshyari.com/en/article/7992752>

Download Persian Version:

<https://daneshyari.com/article/7992752>

[Daneshyari.com](https://daneshyari.com)